Printed Electronic Sensor Array for Mapping Tire Tread Thickness Profiles

Joseph B. Andrews, *Student Member, IEEE*, Peter Ballentine, Jorge A. Cardenas, *Student Member, IEEE*, Chin Jie Lim, Nicholas X. Williams, James B. Summers, Michael A. Stangler, David A. Koester, Steven A. Cummer, *Fellow, IEEE*, and Aaron D. Franklin, *Senior Member, IEEE*

***Abstract*— Tire tread wear is a significant vehicular safety concern; yet, monitoring tread depth (or thickness) still relies on manual detection, which is rarely done by consumers and is time-consuming for service lane technicians. In this paper, we present a fully printed, one-dimensional electrode array that is able to electrically measure the thickness profile of tread across the width of a tire. The sensor array consists of printed millimeter-sized electrodes composed of a hybrid silver nanoparticle-carbon nanotube (CNT) structure. The array is positioned directly against the outside of a tire (simulating a vehicle driving over the sensors). The thickness profile is then determined by applying an oscillating voltage between each of the electrode pairs in the array and measuring the associated electrical response. Correlation between the electrical response and tread depth across a tire is demonstrated for two distinct, measurable parameters: signal reflectance (S11) and impedance. A 2D electrostatic simulation is applied to explain the operation of the sensors and how the differentiation between grooves and tread blocks is possible based on differing electric field attenuation with distance. This printed sensor array shows promise for electrically monitoring tread profiles using relatively low-cost, readily implemented components.**

***Index Terms*— Printed electronics, capacitive sensor, carbon nanotubes, smart tires, Internet of Things.**

I. Introduction

MONITORING tire tread wear is critical for ensuring proper tire traction and vehicle control [1], [2], with staggering safety implications. In the US alone, there are more than 700 deaths and 19,000 injuries each year from tire-related crashes [3]. In these crashes, more than 25 % of the vehicles had tread depth less than 1.6 mm (2/32") [4] – the regulated minimum for safe vehicle handling. In fact, a recent study from the American Automobile Association (AAA) gave evidence for tires being unsafe even at 3.2 mm (4/32"), showing that all-season tires with $\sim$3.2 mm of tread required 87 more feet to stop on wet roads than for new tires on the same vehicle [5].

Manuscript received April 1, 2019; revised May 16, 2019; accepted May 16, 2019. Date of publication May 20, 2019; date of current version September 5, 2019. The associate editor coordinating the review of this paper and approving it for publication was Prof. Alper Bozkurt. *(Corresponding author: Aaron D. Franklin.)*

J. B. Andrews, P. Ballentine, J. A. Cardenas, C. J. Lim, N. X. Williams, S. A. Cummer, and A. D. Franklin are with the Department of Electrical and Computer Engineering, Duke University, Durham, NC 27705 USA (e-mail: aaron.franklin@duke.edu).

J. B. Summers, M. A. Stangler, and D. A. Koester are with Tyrata, Inc., Durham, NC 27701 USA.

Digital Object Identifier 10.1109/JSEN.2019.2918061

The need for sensors to monitor the condition of tires is not new. After the tire pressure-related safety debacle of the Ford Explorer/Firestone Tires in the early 2000s, the U.S. government passed legislation that requires every new vehicle (from 2008 model onward) to be equipped with a tire pressure monitoring system (TPMS) in each tire [6]. In addition to tire pressure regulation, The U.S. government has also defined a legally safe minimum tread depth of 2/32" [7], with encouragement for consumers and commercial fleet managers to be vigilant about monitoring the tread on their tires; unfortunately, this does not generally happen.

While there have been some recent innovations for monitoring tread depth from within the tire [8]–[10], which would be the ultimate solution, these have yet to penetrate the market. And, even when such sensors are available, it will take many years before they are sufficiently ubiquitous to make an appreciable impact on safety. Meanwhile, there is a pressing need for a near-term sensing solution for measuring the tread wear of tires. Some companies have developed products to address this need in the form of drive-over scanners. These systems use lasers and time-of-flight deflection from the tire surface to measure the tread of each tire as a vehicle is driven over the system. While the technology works, the systems are prohibitively expensive ($5k - $20k) and large, leading them to only be used by a select few, typically in service lanes. What is needed is a sensing technology that is capable of similar tread profile measurement in a platform that is lower cost and more readily implemented for widespread use.

Recent demonstration of a tire tread thickness sensor realized using printed carbon nanotubes (CNTs) shows great promise for this sensing need [10]. The use of CNTs provided an enhancement in the sensitivity of the device, while also allowing for the sensor to be printed and thus compatible with low-cost manufacturing techniques. Operation of the sensor relied on electric fields, generated and sensed by the CNT electrodes, passing through the tire and being attenuated with distance in a way that related to the thickness of remaining tread, with some similarities to capacitive proximity sensing [11]–[16]. The demonstration described above [10] holds great promise but was only demonstrated for use from within a tire. The adaptation of this sensing technology into an external tire tread measurement system is the focus of this work.

Ensuring that a sensing technology for monitoring tire tread wear is affordable is imperative and the rapid advancement

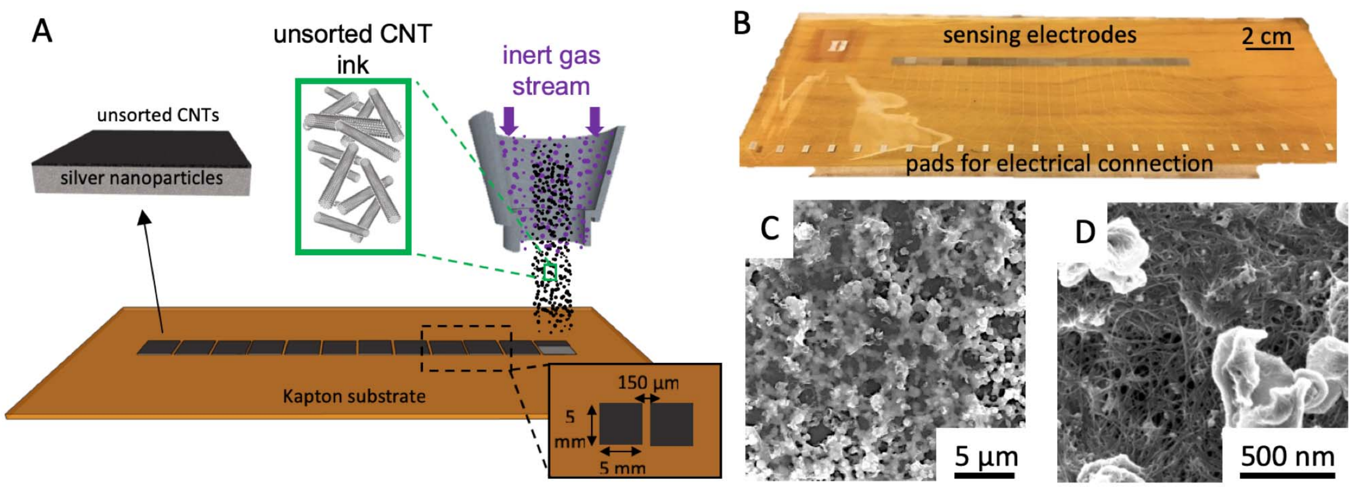

Fig. 1. Design and images of printed sensor array. (A) Schematic illustrating the aerosol jet printing process with an inset profile of an electrode (top-left), consisting of a bottom layer of silver nanoparticles and a top layer of unsorted CNTs. The inset on the bottom right displays the electrode separation and geometry. (B) Photograph of the fully printed sensor array. (C-D) SEM images of the sensing electrodes at different magnifications.

of printing for various materials is an excellent option for low manufacturing cost. Printed electronics have gathered significant research interest in recent years due to the potential for fabricating large area and flexible electronics at a relatively low-cost, particularly when compared to traditional vacuum deposition methods [17], [18]. Additionally, numerous functional inks have been developed, including various nanomaterial-based inks [19]. These novel inks allow for highly functional printed electronic devices, for both sensor [20] and transistor-based applications [21], [22]. It is of note that this work utilizes direct-write printing. This method of electronics fabrication is not low-cost or high-throughput but allows for rapid prototyping and customization. Ultimately, a commercial product would need to be fabricated using roll-to-roll or screen-printing techniques. While non-trivial, it is feasible to translate direct-write printed devices to high-throughput printing methods [23].

In this work, we fabricate fully printed, nanomaterial-based sensor arrays and demonstrate their ability to map tire tread thickness across the width of a tire. The sensor array consists of square millimeter-sized electrodes that are composed of a hybrid composite of printed silver nanoparticles and unsorted single-walled carbon nanotubes (CNTs). An oscillating electric field is applied across adjacent electrodes, while the signal response is measured. This measured signal is shown to correlate with the presence of grooves and tread blocks, with the relative magnitude of the signal corresponding to the thickness of the tread. Using this sensor array, the tread thickness profile of tire can be extracted. A 2D Laplace solver is used to study the electrostatic behavior of the sensors, providing evidence for the mechanism of operation related to changes in electric field attenuation with distance driven by tire material geometry. This successful demonstration of tire tread measurement using an electronic, non-invasive, drive-over sensor array opens the way for tire health monitoring to be done more ubiquitously.

II. Experimental

The sensor array was printed using an aerosol jet printer (AJ300, Optomec Inc.), though the process is adaptable to any number of other printing technologies, such as roll-to-roll gravure printing [23]. In addition to providing a potentially low-cost fabrication scheme, printing the sensor allows for the use of a flexible substrate, which can be bent slightly around the outside of the tire during operation. Aerosol jet printing also enables the controlled deposition of nanomaterials which have been shown to increase the efficacy of the desired sensing scheme [10]. A schematic of the sensor array, along with a photograph, can be seen in Fig. 1A and 1B, respectively. During the aerosol jet printing process, inks composed of nanomaterials dispersed in solvents are ultrasonically atomized to form an aerosol mist. The mist is then carried by an inert nitrogen gas stream to the print head and further aerodynamically focused at the nozzle using a sheath flow of N_2 gas to jet onto the substrate. This process allowed for the printing of both layers, Ag nanoparticles and unsorted CNTs, onto the substrate. The substrate, a 25.4 μm polyimide film (Kapton, Dupont), was first cleaned by sonication in acetone for 5 minutes, followed by sonication in isopropanol for 5 minutes, a rinse using deionized water, and then it was dried using an N_2 gas stream.

The Ag nanoparticle ink (procured from UT Dots, Inc.) contained Ag nanoparticles dispersed at 40 wt. % in a 4:1 mixture of xylene and terpinol. The Ag nanoparticles were printed onto the Kapton substrate in a pattern consisting of twenty-four adjacent 5 by 5 mm square electrodes with a separation distance of 150 μm (pitch of 5.15 mm). Each electrode was connected by a printed lead line to a small rectangular pad, also composed of Ag nanoparticles. These smaller pads were used to electrically connect the sensing electrodes to a vector network analyzer for measurement. The silver nanoparticle samples were printed using a deposition nozzle with a diameter of 100 μm. The sheath and atomizer flow rates for the aerosol jet printer were set to 25 and 20 sccm, respectively. The current used to ultrasonically atomize the silver nanoparticle ink was 320 mA, with the platen temperature held at 60 °C. After printing, the silver nanoparticles were sintered in an oven at 200 °C for 30 minutes.

The unsorted (both metallic and semiconducting) single-walled carbon nanotube ink (P3-CNTs from Carbon Solutions, Inc.) contained 0.5 mg/ml of CNTs dispersed in deionized water. The CNTs were printed directly on top of the Ag nanoparticle electrodes, using a deposition nozzle with a diameter of 150 μm. The sheath and atomizer flow rates for the printing of the CNTs were 35 and 40 sccm, respectively. The current used to ultrasonically atomize the unsorted CNTs was 413 mA, and the platen was held at 60 °C. Like the silver nanoparticles, the unsorted CNTs were sintered at 200 °C for 30 minutes. An SEM image of the composite material can be seen in Fig. 1C-D. Of particular note is the porosity of the silver nanoparticle film, with the CNTs acting as bridges between each nanoparticle. It has been demonstrated that there is a distinct tradeoff that stems from the metallization coverage of the electrode [13], where higher metallization factors lead to higher, more measurable capacitance values, but also lead to smaller penetration depths and sensitivity. Therefore, a porous, yet conductive electrode is key to obtaining appropriate sensitivity with a strong signal-to-noise ratio.

Two distinct electrical parameters were measured and shown to provide the desired tire tread depth profile: signal reflectance (S11) and impedance. Both of these parameters are measurable with an off-the-shelf vector network analyzer (VNA), and the simplicity of the response suggests that a much simpler circuit could be used to drive the sensor array (thus, not relying on an expensive, multipurpose VNA). An SDR Kits DG8SAQ VNA 3E was used for the S11 measurements and a Copper Mountain R60 for the impedance. The measurements were carried out by testing each electrode pair one at a time. An oscillating electric field was applied while simultaneously measuring the reflected signal or the impedance. For the S11 measurements, a frequency range (from 1 to 1000 MHz for S11) was tested at a voltage value of 225 mV rms.

For the initial testing setup, the array was affixed to a pliable piece of balsa wood in order to maintain its structural integrity. The sensor array was then placed against the outside of a tire as seen in Fig. 2A. Wires were soldered to copper tape and fixed on to the connection pads, with the other ends of these wires being connected to a breadboard. The VNA was connected to the breadboard through coaxial components. Additionally, the nearest neighbor electrodes to the active sensing electrodes were held at the same potential (as depicted in Fig. 2B), in order to prevent a loss in electric field outside of the sensing area. The rationale behind this connection scheme is that if the pads directly adjacent to the sensing pads of interest were left at a floating voltage, they could affect the sensing at the location of interest in an unpredictable fashion. Five tests were taken on each set of four electrodes. This measurement scheme was repeated serially across the width of the array to provide the one-dimensional profile of a tire.

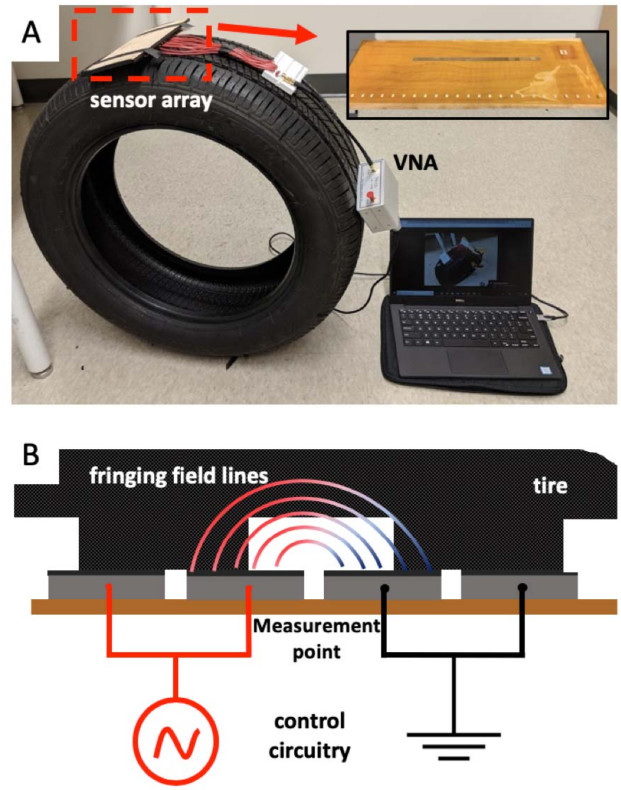

Fig. 2. Initial testing setup and sensor array operation. (A) Photograph of the sensor array placed on the outside of a tire and connected to a VNA. (B) Cross-sectional schematic showing a magnified view of four electrodes in the array against a tire; measurements were taken by having electrodes to one side of the active electrodes ("measurement point") tied to signal while those on the other side were tied to ground. A conceptual illustration of the fringing electric field lines interacting with the tire is also included.

In addition to the simple setup involving the sensor array attached to the tire, a custom test assembly was also designed and constructed for applying a tire onto a sensor array with the same amount of force as will be present in a drive-over application. This test setup provides proof-of-concept demonstration of the ability for the sensor array to map the tread profile for a tire that is being driven directly over its surface (Fig 4). While this demonstration proves the viability of the sensor at high forces, a high-speed automated measuring system was not developed to fully demonstrate the drive over method.

III. Results and Discussion

Tire tread typically has three specific regions of different thickness – the tread, the sipes, and the grooves. The primary indication of tread wear, and thus the most beneficial measurement, is the tread thickness, which is the difference between a tread block and a groove. Therefore, a comparison between the measured signal spectra at each specific critical point is crucial to understanding the operation of the tire array sensor. The spectrum of the signal reflectance with respect to frequency at three distinct tire locations (defined by the position of the measurement point shown in Fig. 2B) is shown in Fig. 3A. The spectra indicate multiple resonances

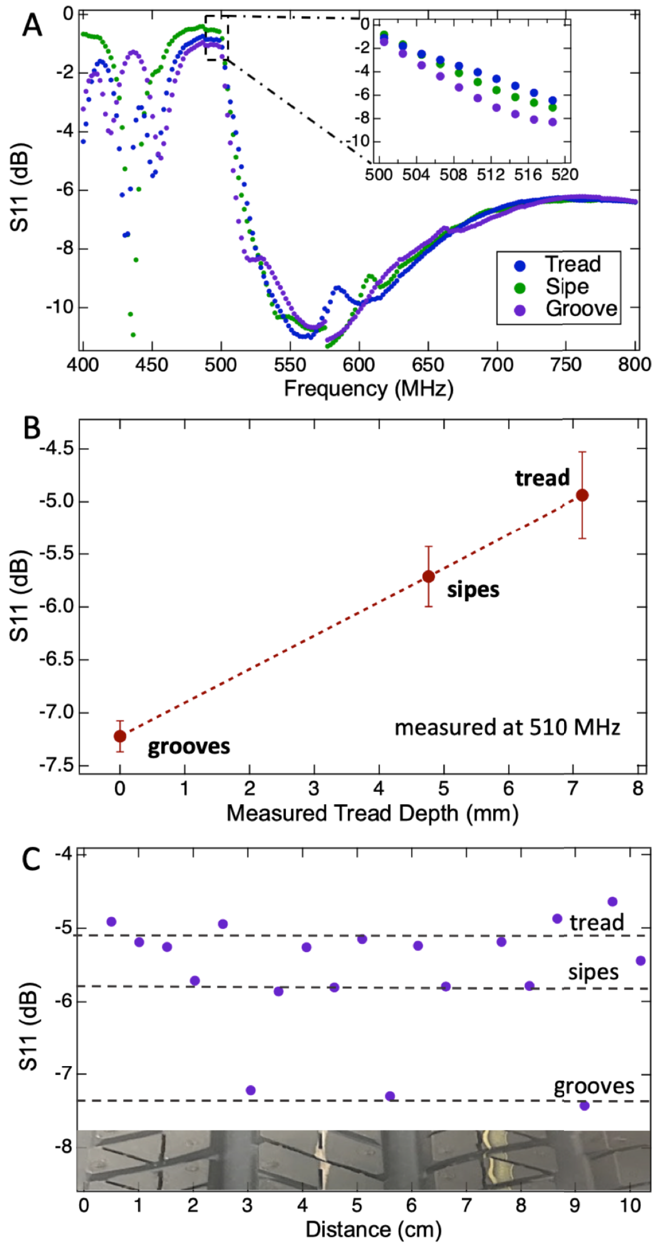

Fig. 3. Operation of sensor array using reflected signal (S11) magnitude. (A) Representative S11 versus frequency response for three sensor measurement points on a tire: full tread, sipes (or minor tread patterns), and the full grooves (0 mm tread depth). Inset shows active sensing frequency range. (B) S11 versus actual tread thickness at three distinct tire positions (actual thickness measured with a tread depth gauge). The correlation is extremely linear ($R^2 > 0.99$) with error bars indicating a 99 % confidence interval from 5 samples taken at each location. (C) Slope-adjusted S11 across the full width of the tire. S11 response is tri-modal, corresponding to full tread, sipes, and grooves. These measurements were taken using a stationary array positioned on the outside of the tire. An inset at the bottom of the plot shows the tire profile as it corresponds (approximately) with the position of the array during the measurements.

within the measured frequency range with the second resonant peak being the most consistent and comparable across each location. However, the reflected signal amplitude at the resonant frequencies is small, due to almost no power being reflected back to the electrodes. Therefore, directly measuring either the resonant frequency or the magnitude at the exact resonant frequency is noisy and highly variable. One way to measure the changes to the resonant frequency with more robustness is to measure the signal reflectance magnitude (S11 in dB) directly above or below that frequency. For example, the frequencies directly at the shoulder of the resonant peak are shown in the inset of Fig. 3A. The trend of decreasing S11 magnitude at each specific frequency, and with respect to decreasing material thickness, was observed. Through these S11 signatures, it was determined that the optimal parameter for the sensor array in this initial testing setup would be the S11 magnitude at 510 MHz.

Next, the S11 magnitude (directly above the shoulder of the resonant peak) was plotted against the actual measured tread depth at each position. The tread depth is defined as the height of rubber material with respect to the grooves. Therefore, the groove height is normalized to 0 mm. The results can be seen in Fig. 3B, showing a direct and linear correlation between the measured S11 and the tire tread depth, with a coefficient of determination value (R^2) being greater than 0.99. The linear correlation validates the hypothesis that the S11 parameter is directly linked to the tire's tread depth at the given sensing frequency. Given the linear relationship, the estimated tread depth and 99% confidence intervals for the grooves, sipes, and tread are 0 ± 0.47 mm, 4.76 ± 0.87 mm, and 7.15 ± 1.30 mm, respectively. Additionally, the fact that the response is linear provides a unique way to calibrate the sensor in real time: the difference in S11 magnitude between the high (tread blocks) and low (grooves) points corresponds to a certain tread depth. This is true even if the specific magnitudes of the measured S11 are different; the difference between high and low will still be consistent and related to overall tread depth.

The full extent of the printed one-dimensional array was tested to provide a profile across the width of the tire. The S11 magnitudes at 510 MHz were correlated with the position of the sensor array on the tire, as seen in Fig. 3C. The data had a tri- modal distribution with the positions of each mode corresponding with a tire feature. It should be noted that the data here was normalized to a slope that existed within the raw dataset. This type of signal drift is often seen in the capacitive proximity sensing due to fluctuations in the environment, therefore, it must be normalized by measuring two known points (tire tread in this case) and subtracting the measured slope from the original data. Additionally, while the measurement technique was consistent across 95% of locations measured, the measurement at 7 cm presented an outlier which has been removed from the plot. Overall, this one-dimensional tire tread map provides a proof-of-concept demonstration of a fully-printed, array being used to measure tire wear.

While the sensor array was operated by monitoring the S11 modulation for different locations across the width of a tire, the sensing mechanism is not attributed to electromagnetic (antenna-like) behavior. The actual frequency at which these sensor electrodes resonate is in the GHz range, meaning the observed shift in S11 is related to changes in the quasi-static fields, including the electric and magnetic fields, which are typically measured as changes in capacitance, inductance, impedance, or reactance. To demonstrate that the measurement

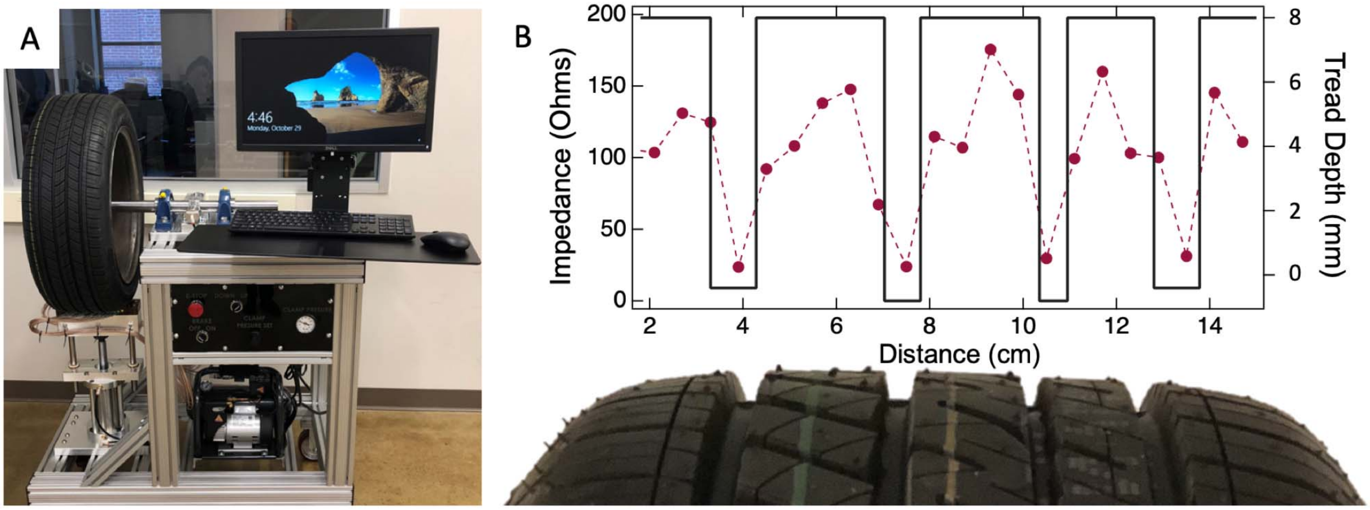

Fig. 4. Operation of sensor array with custom test setup using impedance. (A) Test system with adjustable pneumatic pressure control to simulate pressure from the tire on the sensor surface. System includes 23 channels with automated channel switching and data acquisition. (B) Impedance versus location across width of the tire. For reference, the actual tread depth is displayed using the gray profile corresponding to the right axis, with the groove referenced at 0 mm. Data is aligned with a photo of the tire for illustration purposes.

of the tire profile can be achieved using one of these other parameters, which are less complex to implement than S11, operation of an array using impedance is shown in Fig. 4. This array is measured using the custom testing apparatus shown in Fig. 4A that applies a tire with known physical load to the array to more accurately simulate the operation with a vehicle driving over the array. The data shows that change in impedance is correlated to the tread thickness across the width of the tire (Fig. 4B), just as was observed for S11.

To verify the hypothesis that these sensors are measuring tire tread depth through changes in the electric field over the various sensor locations in the array, we developed and apply a numerical model of the sensor and tire configuration. This model is solely meant for theoretical verification and is not predictive of exact sensor measurements. This model is a 2D cartesian Laplace solver in which a known voltage difference is applied across the sensor electrodes, and the resulting potential distribution is postprocessed with a gradient operator to deliver the 2D electrostatic field distribution. The 2D Laplace equation solver uses a finite difference approximation of the second derivative Laplacian operator with a standard 4-point stencil. The finite difference system of equations is iteratively solved using successive overrelaxation with red-black ordering [24]. The potential of the electrodes is fixed at either one or zero (ground). The potential along the square boundary of the computational domain is also set at zero, and the boundary is set at a sufficiently large distance from the electrodes such that it does not significantly influence the solution. Regions of different electric permittivity can be specified so that the realistic tire tread geometry can be accounted for. Figure 5 shows the electric field direction and magnitude from simulations with a single pair of electrodes that are 5 mm wide and 100 μm thick with a 200 μm spacing. Relative permittivity of the tire rubber was taken to be 6 with everywhere else kept at 1 to represent air. In Fig. 5A, the sensor electrode pair is centered on a tread block of 3 mm thickness, with a groove visible on either side of the tread block. For Fig. 5B, the sensor is centered on a groove, with tread blocks visible on either side. The simulation shows that there is a dramatic difference in the electric field distribution when the electrodes are near the tread versus the groove. With a tread block above the sensor, the electric field is weaker very close to the sensor (upon interaction with the interface of the tire material) and extends nearly uniformly throughout the tread block. Meanwhile, when centered on the groove, the electric field from the sensor is higher throughout the air gap and then dramatically drops once entering the tire rubber.

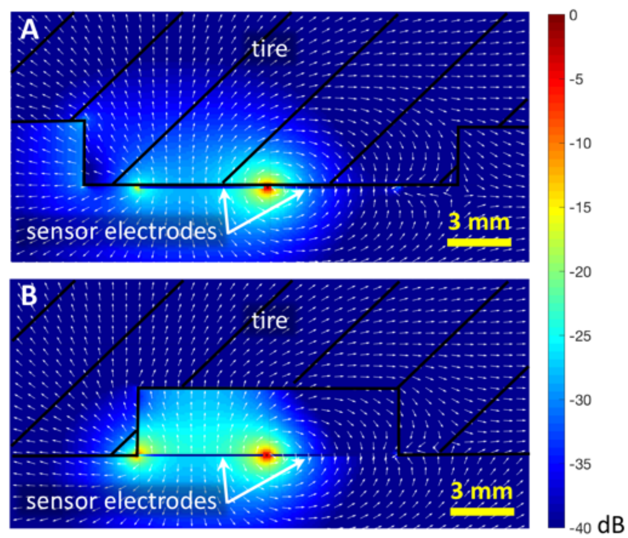

Fig. 5. Simulation of sensor operation. 2D Laplace model showing electric field magnitude (in dB with rainbow scale) and direction. (A) Sensor electrodes (5 mm wide, 200 μm spacing) centered on, and abruptly interfacing with, a tire tread block, showing uniform electric field distribution within the tire material. (B) Sensor electrodes centered on a groove of 3 mm depth, showing disruption of the electric field at the bottom of the groove and thus dependent on the groove/tread depth. Relative permittivity for the tire was 6 and the left electrode was signal with the right electrode grounded.

These significantly different electric field distributions support the hypothesis that the operation of the sensor array is based on these electric field differences for sensors at distinct locations across a tire's surface.

IV. Conclusion

The ability of a low-cost, printed sensor array to measure the tread depth across the width of a tire has been demonstrated. A combination of Ag nanoparticles and CNTs were used for the sensor electrodes, printed onto a Kapton substrate. Demonstration of the sensor array successfully measuring a tire profile was provided using both a simple attachment to the outside of a tire as well as a more advanced testing setup that simulated a tire driving over the array. Using a 2D Laplace solver to simulate the electrostatic fields near the sensor electrodes, the operating mechanism for this sensing technology was confirmed: significant changes in the electric field based on sensor location (e.g., beneath tread or groove). This work provides an encouraging path forward for more widespread implementation of tire tread monitoring to improve safety for all drivers and passengers.

References

[1] NHTSA. (2012). *Tire-Related Factors in the Pre-Crash Phase*. Accessed: Oct. 26, 2018. [Online]. Available: https://crashstats.nhtsa.dot.gov/Api/Public/ViewPublication/811617

[2] NHTSA. (2013). *Safety in Numbers*. Accessed: Oct. 26, 2018. [Online]. Available: https://one.nhtsa.gov/nhtsa/safety1nnum3ers/june2013/SafteyInNumbersJune2013.html

[3] NHTSA Gets Real on Tire Fatalities. (2018). *The Safety Record Blog*. Accessed: Oct. 26, 2018. [Online]. Available: http://www.safetyresearch.net/blog/articles/nhtsa-gets-real-tire-fatalities

[4] J. M. Gitlin. (2018). More Than One in Three Drivers Doesn't Know When Their Tires are Bald. ARS Technica. [Online]. Available: https://arstechnica.com/cars/2018/06/more-than-one-in-three-drivers-dont-know-when-their-tires-are-bald/

[5] AAA Newsroom. (2018). *AAA All-Season Tire Testing*. Accessed: Oct. 26, 2018. [Online]. Available: https://www.aaa.com/AAA/common/AAR/files/Tire-Study-Report.pdf

[6] M. Grayen. (2016). What is the History of Tire Pressure Monitoring Systems?. CARiD. Accessed: Oct. 26, 2018. [Online]. Available: https://www.carid.com/articles/what-is-history-of-tire-pressure-monitoring-systems.html

[7] (2018). *Tire Tech: Tire Specs Explained: Tread Depth*. Accessed: Nov. 30, 2018. [Online]. Available: https://www.tirerack.com/tires/tiretech/techpage.jsp?techid=197

[8] (2017). *Pirelli Connesso*. Accessed: Oct. 26, 2018. [Online]. Available: http://www.pirelliconnesso.com/

[9] Continental. (2016). *Continental AG Fact Book*. Accessed: Oct. 26, 2018. [Online]. Available: https://www.continental-corporation.com/resource/blob/18126/63257ef8799d3e00f73f4fbee18d0b9f/fact-book-2016-data.pdf

[10] J. B. Andrews, C. C. Cao, M. A. Brooke, and A. D. Franklin, "Noninvasive material thickness detection by aerosol jet printed sensors enhanced through metallic carbon nanotube ink," *IEEE Sensors J.*, vol. 17, no. 14, pp. 4612–4618, Jul. 2017.

[11] A. A. Nassr and W. W. El-Dakhakhni, "Non-destructive evaluation of laminated composite plates using dielectrometry sensors," *Smart Mater. Struct.*, vol. 18, no. 5, 2009, Art. no. 055014.

[12] A. A. Nassr and W. W. El-Dakhakhni, "Improved interdigital sensors for structural health monitoring of composite retrofit systems," *J. Reinforced Plastics Compos.*, vol. 30, no. 7, pp. 621–629, 2011.

[13] J. Jiao, L. Li, B. Wu, and C. He, "Novel capacitive proximity sensors for assessing the aging of composite insulators," *Sens. Actuators A, Phys.*, vol. 253, pp. 75–84, Jan. 2017.

[14] T. Chen and N. Bowler, "Analysis of a concentric coplanar capacitive sensor for nondestructive evaluation of multi-layered dielectric structures," *IEEE Trans. Dielectr. Electr. Insul.*, vol. 17, no. 4, pp. 1307–1318, Aug. 2010.

[15] N. Li, H. Zhu, W. Wang, and Y. Gong, "Parallel double-plate capacitive proximity sensor modelling based on effective theory," *AIP Adv.*, vol. 4, no. 2, 2014, Art. no. 027119.

[16] X. Hu and W. Yang, "Planar capacitive sensors—Designs and applications," *Sensor Rev.*, vol. 30, no. 1, pp. 24–39, 2010.

[17] P. Rosa, A. Câmara, and C. Gouveia, "The potential of printed electronics and personal fabrication in driving the Internet of Things," *Open J. Internet Things*, vol. 1, no. 1, pp. 16–36, 2015.

[18] S. R. Forrest, "The path to ubiquitous and low-cost organic electronic appliances on plastic," *Nature*, vol. 428, pp. 911–918, Apr. 2004.

[19] E. B. Secor and M. C. Hersam, "Emerging carbon and post-carbon nanomaterial inks for printed electronics," *J. Phys. Chem. Lett.*, vol. 6, no. 4, pp. 620–626, 2015.

[20] J. B. Andrews, J. A. Cardenas, J. Mullett, and A. D. Franklin, "Fully printed and flexible carbon nanotube transistors designed for environmental pressure sensing and aimed at smart tire applications," in *Proc. IEEE SENSORS*, 2017, pp. 1–3.

[21] C. Cao, J. B. Andrews, and A. D. Franklin, "Completely printed, flexible, stable, and hysteresis-free carbon nanotube thin-film transistors via aerosol jet printing," *Adv. Electron. Mater.*, vol. 3, no. 5, 2017, Art. no. 1700057.

[22] J. A. Cardenas *et al.*, "In-place printing of carbon nanotube transistors at low temperature," *ACS Appl. Nano Mater.*, vol. 1, no. 4, pp. 1863–1869, 2018.

[23] P. H. Lau *et al.*, "Fully printed, high performance carbon nanotube thin-film transistors on flexible substrates," *Nano Lett.*, vol. 13, no. 8, pp. 3864–3869, 2013.

[24] W. H. Press, S. H. Teukolsky, W. T. Vetterling, and B. P. Flannery, *Numerical Recipes: The Art of Scientific Computing*. New York, NY, USA: Cambridge Univ. Press, 2007.

Joseph B. Andrews received the B.S. degree in electrical engineering from the University of South Carolina in 2015. He is currently pursuing the Ph.D. degree in electrical engineering with Duke University.

Prior to the Ph.D. degree, he was a DAAD-Rise Fellow, conducting research on carbon nanotube composite materials in Jena, Germany. His current research interests include printed electronic systems and sensors with an emphasis on the Internet of Things and biosensor applications. He has received many awards throughout his Ph.D. degree including the James B. Duke Fellowship, the Ruth L. Kirschstein National Research Service Award (F31) from NIH, and the IEEE SENSORS Conference Top Student Paper Award in 2017.

Peter Ballentine is a currently pursuing the bachelor's degree with Duke Kunshan University, Kunshan, China. He is majoring in material science and chemistry.

Prior to the bachelor's degree, he was an Intern with Duke University researching printed electronics. After his first year attending Duke Kunshan University, he returned to Duke University, where he is currently conducting research on carbon nanotube materials with an emphasis on applications in printed electronics.

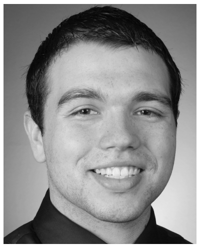

Jorge A. Cardenas received the B.S.E. degree in electrical engineering from Arizona State University in 2016. He is currently pursuing the Ph.D. degree in electrical engineering with Duke University.

He is currently with Army Research Labs investigating the photonic curing of printed electronic inks and devices. His current research interests include printed electronics and materials with an emphasis on the additive printing of low-cost, flexible electronics using nanomaterial-based inks that are compatible with low-temperature processing. He was a recipient of the National Science Foundation's Graduate Research Fellowship and the James B. Duke Fellowship.

Chin Jie Lim was born in Singapore in 1993. He received the B.S. degree in electrical and computer engineering and the B.S. degree in economics from Duke University in 2018.

He is currently working as an Associate with the Singapore Economic Development Board.

Nicholas X. Williams received the B.S. degree in materials science from Johns Hopkins University in 2012. After graduation, he was a battery chemist in San Francisco. He is currently pursuing the Ph.D. degree in electrical engineering with Duke University.

His research focuses on printed electronics, including electronic ink development, and sensor design and fabrication with a specialization on biosensor applications.

James B. Summers received the B.S. degree in electrical engineering from Valparaiso University in 2004 and the M.S. degree in electrical engineering from Case Western Reserve University in 2007.

He is a senior engineer with experience in early- and mid-stage development of novel technologies. Prior to working with Tyrata, he implemented manufacturing-scale test systems for thermoelectric coolers and assemblies.

Michael A. Stangler received the B.S. degree in mechanical engineering from North Carolina State University in 2018.

His prior experience includes working at Wolfspeed as a Power Intern, developing SiC processes. He is currently working with Tyrata as a Product Engineer, specializing in sensor design, layout and fabrication, and test fixture development.

David A. Koester received the B.S. degree in ceramic engineering from Iowa State University and the M.S. degree in materials science from North Carolina State University.

He is with a start-up company and an early-stage product development executive with over 30 years of experience in maturing and commercializing nascent technologies, engineering management, new business development, and technical sales. Prior to joining Tyrata, he was the VP of Business Operations with Zenalux Biomedical, developing novel spectroscopy techniques for cancer detection. He was a Co-Founder of Nextreme Thermal Solutions, where he developed thin-film thermoelectric technology. Nextreme was sold to Laird in 2013, where he served as VP of Technology with the Engineered Thermal Systems business unit. Prior to Nextreme, he was a Principal and Founding Member of the Technical Staff with Cronos Integrated Microsystems, where he developed MEMS products for optical switching and attenuation. Cronos was sold to JDS Uniphase in 2000. He holds 11 patents and has authored or coauthored over 20 technical articles and peer-reviewed articles.

Steven A. Cummer (F'11) received the B.S., M.S., and Ph.D. degrees in electrical engineering from Stanford University in 1991, 1993, and 1997, respectively.

He is currently the William H. Younger Professor of Electrical and Computer Engineering with Duke University. He spent two years with the NASA Goddard Space Flight Center as a National Research Council Post-Doctoral Research Associate from 1997 to 1999 before joining Duke University. He has written or coauthored more than 230 papers in refereed journals. He received a Presidential Early Career Award for Scientists and Engineers (PECASE) in 2001. He is a Fellow of the American Geophysical Union. His current research interests span a variety of topics in complex materials for controlling electromagnetic and acoustic wave propagation, and in geophysical remote sensing with a focus on lightning and atmospheric electricity.

Aaron D. Franklin (M'09–SM'15) received the B.S.E. degree in electrical engineering from Arizona State University in 2004 and the Ph.D. degree in electrical engineering from Purdue University in 2008.

In 2004, prior to pursuing the Ph.D. degree, he was a Component Design Engineer with Intel Corporation. After the Ph.D. degree, he was a Research Staff Member with the IBM T. J. Watson Research Center for six years. In 2014, he joined the Department of Electrical and Computer Engineering and Chemistry, Duke University, as an Associate Professor. His current research interests include nanomaterials in high-performance nanoelectronic devices, nanomaterial inks for low-cost printed electronics, and harnessing nanomaterial sensitivity in bioelectrical systems. Applications of his work cover a broad range of areas, including nanoelectronics, sensors and circuits for the Internet-of-Things (IoT), low-voltage transistors, electrical energy conversion/storage, and biosensors.

Dr. Franklin has served on organizing committees of symposia for various meetings of the Materials Research Society (MRS), the Applied Physics Society (APS), the American Chemical Society (ACS), and the IEEE. He was the Technical Program Chair of the 2017 75th Device Research Conference (DRC) and the Subcommittee Chair of Nano Device Technology (NDT) of the IEEE International Electron Devices Meeting (IEDM) in 2017.